Earth and Planetary Science Letters xxx (2011) xxx–xxx

Contents lists available at SciVerse ScienceDirect

Earth and Planetary Science Letters

journal homepage: www.elsevier.com/locate/epsl

Climate information imprinted in oxygen-isotopic composition of precipitation in Europe

P.M. Langebroek *, M. Werner, G. Lohmann

Alfred Wegener Institute for Polar and Marine Research (AWI), Bremerhaven, Bussestrasse 24, D-27570 Bremerhaven, Germany

ARTICLE INFO

Article history:
Received 1 April 2011
Received in revised form 20 July 2011
Accepted 10 August 2011
Available online xxxx

Editor: G. Henderson

Keywords:
$\delta^{18}O$ of precipitation
NAO
Europe
Bunker Cave
ECHAM5
speleothem

ABSTRACT

In this study we analyze the interannual variability of the oxygen-isotopic composition of winter precipitation ($\delta^{18}O_{prec}$) over Europe and investigate its related climate information. For this purpose we compare winter temperature, precipitation and $\delta^{18}O_{prec}$ modeled by the atmospheric general circulation model ECHAM5-wiso with different observational datasets over Europe. In general the model and data results are very similar for the present-day climate and the modeled $\delta^{18}O_{prec}$ is matching the Global Network of Isotopes in Precipitation station data. ECHAM5-wiso only slightly underestimates the temperatures over Europe (mean difference ~0.4 °C). The mean European precipitation amount is very similar (~85 mm/month), however in central western Europe the modeled precipitation is overestimated by up to 30 mm/month. We also evaluate the large-scale circulation associated with the regional $\delta^{18}O_{prec}$ values. By correlating the North Atlantic Oscillation (NAO) index to modeled $\delta^{18}O_{prec}$ fields, we show that the NAO pattern is most pronouncedly imprinted in $\delta^{18}O_{prec}$ over central western Europe, consistent with observations. We demonstrate for an example location near a stalagmite site in central Germany, how local isotope-related climate variables are related to large-scale European climate variability. We find that, in both the model results and the data, present-day winter variability of local $\delta^{18}O_{prec}$ is strongly related to atmospheric circulation (remote sea-level pressure fields) and much less to the local and remote temperature or precipitation fields. The simulated correlation pattern resembles the NAO pattern, but is tilted to the east due to the combined effect of temperature and precipitation.

1. Introduction

Over the last decades many different kinds of terrestrial records (e.g. ice cores, lake sediments, tree rings and speleothems) have been used to derive information on past climate changes. One of the most commonly used proxies for these paleoclimate reconstructions is the ratio of oxygen isotopes ($\delta^{18}O$, relative deviation in ‰ from a standard) measured in the different climate archives (e.g., Kress et al., 2010; McDermott, 2004; Petit et al., 1999). $\delta^{18}O$ in the archives depends strongly on $\delta^{18}O$ in precipitation, $\delta^{18}O_{prec}$, which in turn is used as a proxy for past temperature and precipitation changes.

In this study we evaluate simulated $\delta^{18}O_{prec}$ and related climate indices (temperature, precipitation and sea-level pressure) over Europe. We concentrate on Europe because its climate conditions are captured in many observational datasets and archived in several different climate records (e.g., Andersson et al., 2010; Baldini et al., 2006; Kress et al., 2010; McDermott, 2004).

European interannual climate variability is strongly modulated by the North Atlantic Oscillation (NAO, e.g., Hurrell, 1995a). This mode of atmospheric variability controls the strength and direction of the westerly winds over Europe and the North Atlantic. The NAO index is defined as a difference in sea-level pressure (SLP) between the Iceland Low and Azores High pressure systems (e.g., Jones et al., 1997; Walker and Bliss, 1932). During the positive phase of the NAO the strong pressure difference causes a more intense atmospheric circulation and strong westerly winds. The influence of the NAO is most pronounced for boreal winter. A positive NAO results in relatively high winter temperatures in Central Europe and frequent precipitation. In a negative NAO phase the westerlies weaken and storm tracks are shifted to the south, leading to colder winter temperatures and less precipitation in Central Europe (e.g., Hurrell, 1995a).

One of the natural archives recording past climate conditions is stalagmites. The $\delta^{18}O$ signal recorded in the stalagmites calcite depends on the $\delta^{18}O$ of the drip water feeding the stalagmite and on the isotopic fractionation process during calcite precipitation. The latter depends largely on the cave temperature and on other conditions in the cave, while the former carries the $\delta^{18}O_{prec}$ climate information to the cave. On its way to the dripsite, the $\delta^{18}O$ is altered by processes in the overlying vegetation, soil and karst. For a comprehensive

* Corresponding author at: Bjerknes Centre for Climate Research, Bergen, Norway.
E-mail address: petra.langebroek@uni.no (P.M. Langebroek).

0012-821X/$ – see front matter © 2011 Elsevier B.V. All rights reserved.
doi:10.1016/j.epsl.2011.08.049

overview on the reconstruction of paleo-climate from stalagmites we refer to McDermott (2004) and Lachniet (2009).

Within the DAPHNE project ('Dated speleothems archives of the paleoenvironment') several European stalagmite records and sites are investigated. One of these cave systems, Bunker Cave in Germany, has been well monitored over the last 5 yrs (Riechelmann, 2010). The cave temperature is recorded and at several locations in the cave the amount and $\delta^{18}O$ values of the dripping water and the calcite precipitates are measured. Furthermore the $\delta^{18}O$ soil water and the pCO_2 of soil air are evaluated, and the amount and $\delta^{18}O$ of precipitation above the cave are registered. Because of this relatively long period of intensive monitoring, Bunker Cave has been chosen as the example location for a Drip Water Model, describing the processes in the soil, karst and cave that are modifying the climate signal recorded by the stalagmites (Wackerbarth et al., 2010). This last study furthermore shows that the $\delta^{18}O$ measured in the Bunker Cave stalagmite records is mainly influenced by the precipitation in the boreal winter months, as these months comprise the highest infiltration of precipitation into the cave system.

Because European winter precipitation and temperature are mostly modulated by the NAO, the question that immediately arises is whether the NAO is imprinted in the climate parameters recorded at Bunker Cave. Turning this question around, we investigate in this study in a more general way the isotope-related climate variables that best capture the NAO pattern and in which European region this correlation is most pronounced.

To answer these questions we simulate the present-day climate with an atmospheric general circulation model (ECHAM5). In order to better compare the model results directly to proxy records, we enhanced the model by stable water isotope diagnostics (ECHAM5-wiso). We first evaluate how well the climate variables, temperature, precipitation amount, $\delta^{18}O_{prec}$ and sea-level pressure (SLP), are modeled by comparing the European results to different observational datasets from the European Centre for Medium-Range Weather Forecasts (ECMWF-ERA40, Uppala et al., 2005) and the International Atomic Energy Agency/World Meteorological Organization — Global Network of Isotopes in Precipitation (GNIP) (IAEA/WMO, 2006). The NAO-relation to European $\delta^{18}O_{prec}$, precipitation and temperature fields is examined to retrieve regions where the variables are most strongly NAO dominated.

In order to assess how representative a local $\delta^{18}O$ record is for climate variations we focus on the example region of Bunker Cave. Variations encoded in the Bunker Cave speleothem $\delta^{18}O$ are primarily the result of fluctuations in $\delta^{18}O_{prec}$ modified by soil, karst and cave processes (Wackerbarth et al., 2010). In turn, local variations in $\delta^{18}O_{prec}$ are often interpreted as fluctuations in temperature or precipitation (e.g., Lachniet, 2009; Rozanski et al., 1993). We analyze how strong the interannual variability in the local temperatures, precipitation amounts and $\delta^{18}O_{prec}$ values is related to variations in large-scale atmospheric circulation. We test if SLP fields, as part of the large-scale atmospheric circulation, are better predictors for local $\delta^{18}O_{prec}$ variability than (remote) temperature or precipitations changes.

To show that our results are not artifacts of the (ECHAM5-wiso) model we apply all methods also on the observational datasets and compare the resulting patterns and relationships.

Although we chose a particular site in central western Europe in this example, the presented method can be applied on other locations containing (paleo) records.

2. Methods

We first briefly describe the datasets and the climate model used in this study. Hereafter, we explain the experimental set-up of the performed simulations. In the last sections of this chapter we justify the set of climate parameters we selected and explain on which seasons and time periods we focus.

2.1. Datasets

The first dataset for our study stems from the Global Network of Isotopes in Precipitation (GNIP). It contains temperature and precipitation values and provides the additional variable of oxygen-isotopic composition of precipitation (commonly given in delta notation, $\delta^{18}O_{prec}$). GNIP was initiated by the International Atomic Energy Agency (IAEA), in cooperation with the World Meteorological Organization (WMO) in 1958. Since it became operational in 1961, over 800 meteorological stations all over the world have collected monthly mean samples of temperature, precipitation and/or $\delta^{18}O_{prec}$ (IAEA/WMO, 2006). In Europe approximately 150 stations provide monthly-mean $\delta^{18}O_{prec}$ values of at least one year.

The second suite of data we use is the ECMWF reanalysis dataset ERA40 (Uppala et al., 2005). This dataset contains globally gridded values of climate variables such as temperature, precipitation, evaporation and sea-level pressure, which are reconstructed by means of sophisticated interpolations from a large set of instrumental measurements and satellite data. ERA40 covers the period from September 1957 to September 2002 (exactly 45 yrs), with a six-hourly temporal resolution for many of the parameters. The spatial resolution is approximately 1° by 1° (~100 by 100 km).

To illustrate the small-scale climate features that are not captured by the coarser ERA40 grid size, we employ a third dataset, the German Weather Service (Deutscher Wetterdienst, DWD). This dataset contains monthly mean temperature and precipitation from over 500 stations in Germany.

2.2. ECHAM5-wiso

ECHAM5 is the fifth generation of an atmospheric general circulation model developed at the Max-Planck-Institute in Hamburg (Germany). It was thoroughly tested under present-day conditions (e.g., Roeckner et al., 2003, 2006) and used for the Intergovernmental Panel on Climate Change 4th Assessment Report (Randall et al., 2007). We enhanced the ECHAM5 model by including a water isotope module in the model's hydrological cycle (this model version is named ECHAM5-wiso hereafter), following the work of Joussaume et al. (1984), Jouzel et al. (1987) and Hoffmann et al. (1998). The isotopic ratio within different water reservoirs depends on several climate parameters, such as temperature and humidity. ECHAM5-wiso computes in detail isotopic changes within the entire hydrological cycle, from ocean evaporation through cloud condensation and precipitation (rain- and snowfall) to surface water runoff. For more details on the isotopic enabled ECHAM5-wiso model we refer to Werner et al. (2011). In this study, we focus on the isotopic values of precipitation $\delta^{18}O_{prec}$ as these can best be compared to the measured GNIP $\delta^{18}O$ values.

2.3. Experimental set-up

With the ECHAM5-wiso model we performed a present-day experiment using observed monthly-mean sea-surface temperatures and sea-ice cover for the time period 1954–1999 (Atmospheric Model Intercomparison Project (AMIP)-style forcing, Gates et al., 1999). The $\delta^{18}O$ values of the ocean surface waters were set to observed modern values, derived from the global gridded dataset compiled by LeGrande and Schmidt (2006). The surface waters of large lakes were set to a constant value of 0.5‰. The ECHAM5-wiso model ran in a relatively high resolution, T106L31, which corresponds to a horizontal resolution of approximately 1.1° by 1.1°, and 31 layers in the vertical. The climate model was forced by sea-surface temperatures and sea-ice cover only, leaving the atmospheric circulation free to evolve. As a consequence the modeled climate of a specific month and year cannot be directly compared to the corresponding monthly mean value in any observational dataset. When comparing model

Please cite this article as: Langebroek, P.M., et al., Climate information imprinted in oxygen-isotopic composition of precipitation in Europe, Earth Planet. Sci. Lett. (2011), doi:10.1016/j.epsl.2011.08.049

results with data, rather long-term mean values and variations shall be applied.

2.4. Selection of climate parameters and time period

Temperature and precipitation are commonly measured climate variables, sea-level pressure (SLP) describes large-scale climate patterns and $\delta^{18}O$ is recorded in many paleoarchives. GNIP, ERA40 and DWD datasets provide observed monthly or six-hourly mean values of these parameters and the ECHAM5-wiso results have an even higher temporal resolution.

On interannual timescales European climate is strongly influenced by the NAO (e.g., Hurrell, 1995a), which is most pronounced in boreal winter. Consequently, we select only the winter months (December, January and February) for all parameters. Winter temperature of 1980, for example, consists of the mean temperature of December 1979, January 1980 and February 1980. The calculated mean winter $\delta^{18}O_{prec}$ values are additionally weighted by the monthly amount of precipitation.

We select the period of 1959 to 1999 for our comparison, which is long enough to represent the mean climate state. The ERA40 dataset and the ECHAM5-wiso simulation both cover this full time span of 41 yrs. For the DWD data, 201 stations recorded continuous temperature records and 396 stations precipitation data over this period. Unfortunately, the number of European GNIP stations offering continuous coverage of this time span is limited. Therefore, for the model-data $\delta^{18}O_{prec}$ comparison we average the GNIP $\delta^{18}O_{prec}$ values into three subsets: stations containing less than 5 yrs of winter data (154 stations), 5 or more years of winter data (55 stations) and 10 or more years of $\delta^{18}O_{prec}$ winter data (43 stations). The table in the Supplementary materials shows all long-term winter mean European GNIP values.

2.5. Statistics of results

All correlation coefficients and linear regressions stated in this study are statistically significant (p-values $\ll$ 1e-3) and our error analyses show a maximum error of around 10%.

3. Evaluation of datasets and model results

3.1. European $\delta^{18}O_{prec}$

The comparison of modeled versus measured $\delta^{18}O_{prec}$ data is hampered by the relatively small number of GNIP measurements available for a longer time period. However, when we compare all available GNIP $\delta^{18}O_{prec}$ to the simulated ECHAM5-wiso $\delta^{18}O_{prec}$ we find a very good resemblance between the two (Fig. 1). Lighter $\delta^{18}O_{prec}$ are found in Scandinavia and in the Alps and heavier values on the coasts of Spain and in the Mediterranean. The correlation between all GNIP stations with data of 5 yrs or more and the corresponding ECHAM5-wiso $\delta^{18}O_{prec}$ is relatively high (Fig. 1b, $r^2 \sim 0.8$). The largest deviations from the GNIP measurements occur for strongly depleted alpine $\delta^{18}O_{prec}$ values, where ECHAM5-wiso underestimates the depletion with up to 3‰. This mismatch can probably be explained by the model's incapability of resolving topographic features smaller than a grid box (~100 km), such as the alpine mountain ridges and slopes. Taking the winter mean values over a randomly chosen 5-year period of simulated $\delta^{18}O_{prec}$ instead of the presented mean over 41 yrs gives a very similar distribution pattern and correlation to GNIP data (not shown).

3.2. European temperature and precipitation

Fig. 2 shows the mean winter temperatures and precipitation of ERA40 and ECHAM5-wiso for the period 1959–1999. The simulated temperature pattern is very similar to the ERA40 temperatures, with, as expected, coldest temperatures over Scandinavia and warmest temperatures in the Mediterranean. The analyzed ERA40 and ECHAM5-wiso datasets have a similar spatial resolution. Therefore, we can directly compare the model results to the dataset and find a correlation (r^2) of 0.97. Nevertheless, the model computes slightly lower winter temperatures than ERA40 (European mean of 3.4 °C versus 3.8 °C for ERA40). The cold bias is most extreme over Scandinavia.

The simulated precipitation pattern also shows many similarities to the distribution of the ERA40 precipitation (Fig. 2c and d), with European mean values of 88 mm/month for ECHAM5-wiso and 80 mm/month for ERA40. The largest amount of precipitation is

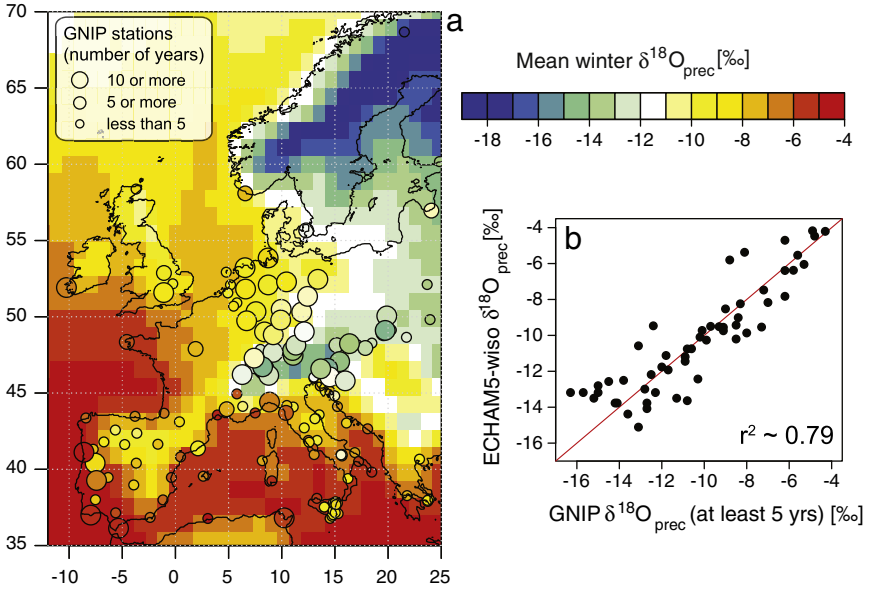

Fig. 1. (a) Winter mean $\delta^{18}O_{prec}$ of GNIP stations (colored circles) and ECHAM5-wiso (background pattern). ECHAM5-wiso values are averaged over 1959–1999. Larger circles indicate longer time series of GNIP measurements. (b) Correlation between GNIP $\delta^{18}O_{prec}$ of stations that includes at least 5 yrs of data and corresponding ECHAM5-wiso $\delta^{18}O_{prec}$ values. The red line indicates the 1:1 line. (For interpretation of the references to color in this figure legend, the reader is referred to the web version of this article.)

Please cite this article as: Langebroek, P.M., et al., Climate information imprinted in oxygen-isotopic composition of precipitation in Europe, Earth Planet. Sci. Lett. (2011), doi:10.1016/j.epsl.2011.08.049

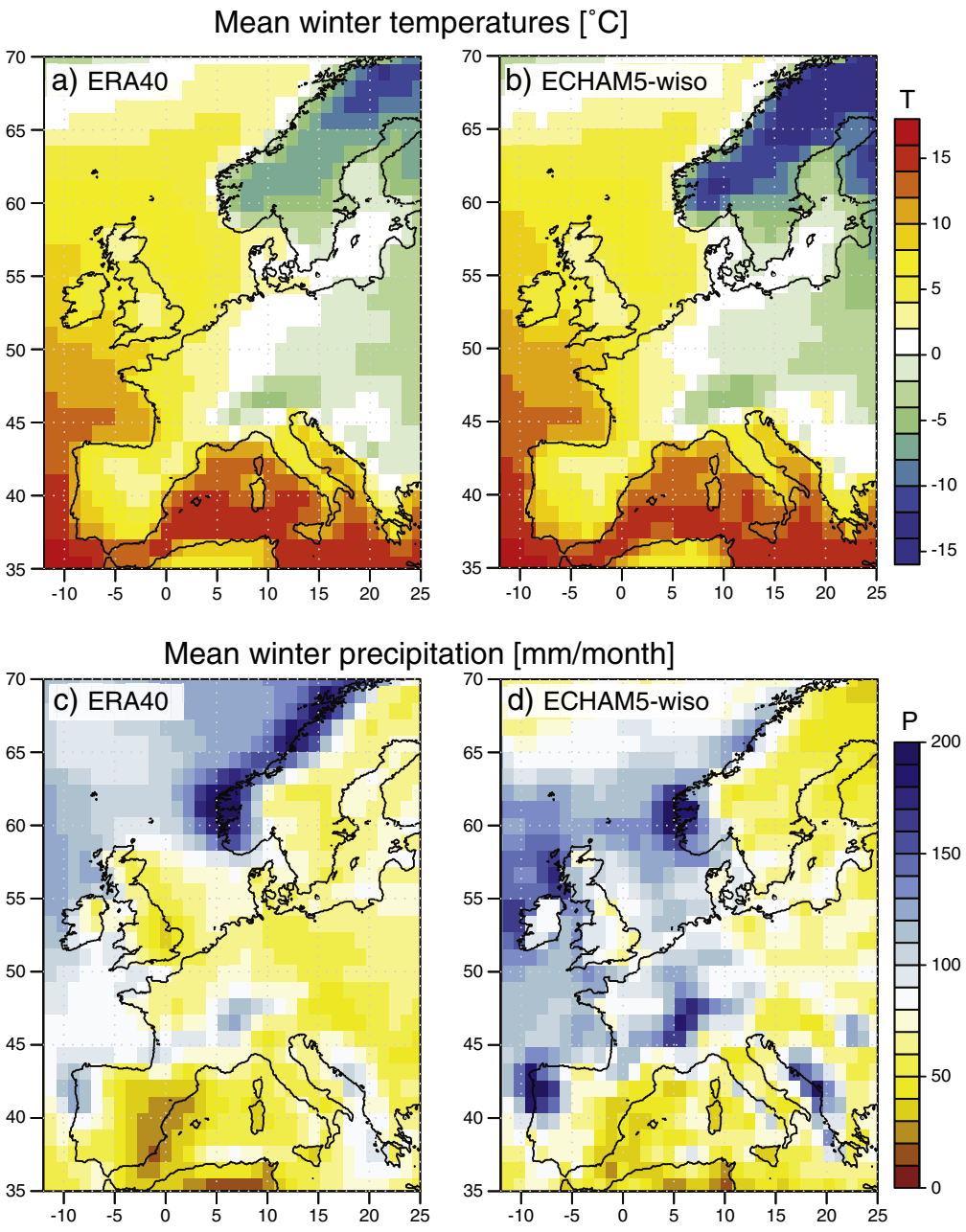

Fig. 2. Mean winter temperature (a and b) and precipitation amount (c and d) over Europe from ERA40 (a and c) and ECHAM5-wiso (b and d). Results are averaged over 1959–1999.

recorded at the western coast of Norway, whereas the driest areas can be found in Spain and the Mediterranean. However, the ECHAM5-wiso results show many wetter areas along the entire Atlantic coast and central Europe receives considerably more precipitation than recorded by the ERA40 data. The correlation ($r^2 = 0.41$) is therefore less than for temperature. Hagemann et al. (2006) find a similar small underestimation of temperature and overestimation of precipitation after comparing ECHAM5 (without water isotope diagnostics) precipitation and temperature over the Danube and Baltic Sea catchment areas to observational datasets. They suggest that the overestimation of precipitation over the oceans might be related to insufficient atmospheric absorption of solar radiation by aerosols, water vapor or clouds.

To investigate how well ERA40 captures very small scale climate features, we compare local DWD station data to the ERA40 dataset in western central Europe (Fig. 3). The DWD temperatures correspond well to the ERA40 grid box in which they are located ($r^2 = 0.49$). In contrast, the DWD precipitation data shows large deviations from the ERA40 dataset ($r^2 = 0.07$). Comparing the same data selecting a shorter and different time period (1988–1994) does not alter these results (not shown). The difference in precipitation between local station data and gridded precipitation (such as ERA40 or the ECHAM5-wiso model results) is most likely due to the large dependence of precipitation on local factors (e.g. elevation and surface slope).

3.3. Sea-level pressures and NAO

Both the Icelandic Low and the Azores High pressure systems are clearly visible in the mean winter SLP patterns of ERA40 and ECHAM5-wiso (Fig. 4). The ECHAM5-wiso SLP pattern is very similar to the ERA40 SLP distribution. However, ECHAM5-wiso computes a slightly less negative low pressure around Iceland and overestimates

Please cite this article as: Langebroek, P.M., et al., Climate information imprinted in oxygen-isotopic composition of precipitation in Europe, Earth Planet. Sci. Lett. (2011), doi:10.1016/j.epsl.2011.08.049

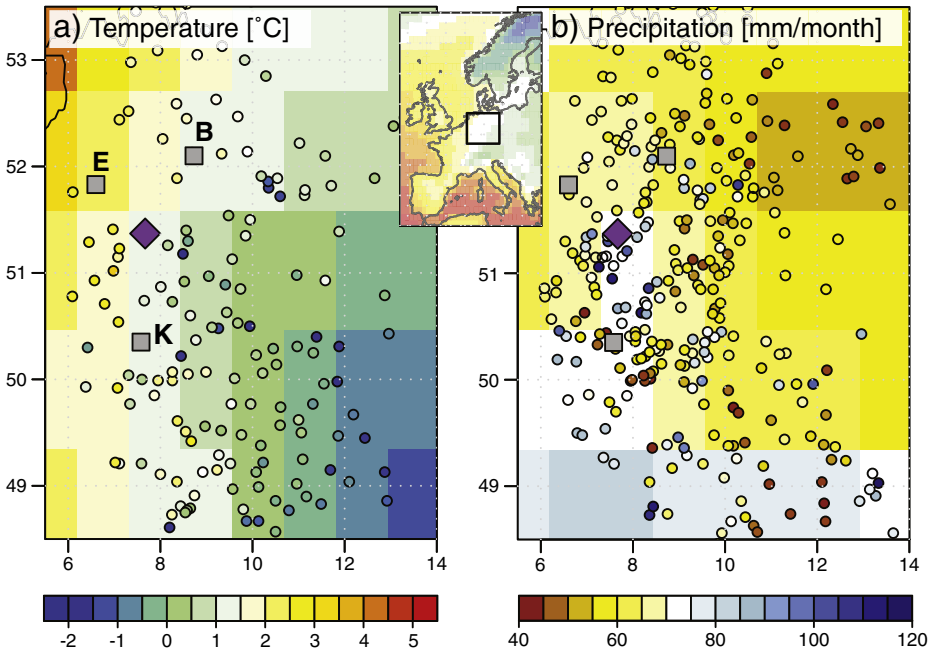

Fig. 3. Mean winter temperature (a) and precipitation amount (b) over Germany from ERA40 (background) and DWD (circles). Results are averaged over 1959–1999. Purple diamond indicates Bunker Cave and the three gray squares locate the GNIP stations closest to Bunker Cave: B (Bad Salzuflen), E (Emmerich) and K (Koblenz). (For interpretation of the references to color in this figure legend, the reader is referred to the web version of this article.)

the high pressure in south-western Europe (difference ~4 hPa). Also, the modeled SLPs over eastern Europe are up to 5 hPa lower than inferred from ERA40.

We perform principal component analyses on the ERA40 and ECHAM5-wiso SLP fields in order to investigate the NAO signal in our data and model results. The spatial pattern of the first EOF of SLPs is very similar for both ERA40 and ECHAM5-wiso (not shown). The temporal evolution of the ERA40 SLP patterns, the ERA40-derived NAO index, follows the same positive and negative NAO phases as Hurrell's December to March station-based NAO index (Hurrell, 1995b). The NAO index derived from ECHAM5-wiso SLPs has a different timing of the positive and negative phases than the real NAO index. This is due to the fact that the simulated atmosphere has internal variability and synoptic-scale features deviate from the observed atmospheric circulation for a specific calendar period.

In order to investigate in which European regions winter temperature, precipitation amount and $\delta^{18}O_{prec}$ are most influenced by the NAO, we correlate our simulated NAO index to the corresponding ECHAM5-wiso variables (Fig. 5). Modeled temperature and $\delta^{18}O_{prec}$ variations are strongly correlated to the NAO in central western Europe. In contrast, ECHAM5-wiso precipitation shows a strong dipole with high positive correlations in northern Europe and high negative correlations in the south. Our simulated correlation patterns between NAO and climate variables are very similar to the relationships found in data (e.g., Hurrell, 1995a). Furthermore, our ECHAM5-wiso results confirm that the imprint of NAO in $\delta^{18}O_{prec}$ values is most pronounced in central western Europe, as previously suggested for GNIP data (Baldini et al., 2008; Field, 2010).

4. Correlation between local and large-scale climate parameters

Because local climatic conditions can be so sensitive to regional variations of small-scale parameters (e.g. topography), they are often difficult to model exactly. However, local climate is almost always also related to large-scale atmospheric patterns, which are generally quite persistent and stationary. Hence, in this section we analyze the relationships between the local temperature, precipitation and $\delta^{18}O_{prec}$ to SLPs over Europe and the North Atlantic. SLPs indicate the main climate pattern near the surface and are therefore often applied as a climate predictor (e.g., Dima and Lohmann, 2004; Hurrell, 1995a; Hurrell and Deser, 2010). We apply the same correlation analysis on both ERA40 reanalysis data and the ECHAM5-wiso modeled variables and compare the computed correlation patterns. If the patterns in the model results resemble the patterns found in

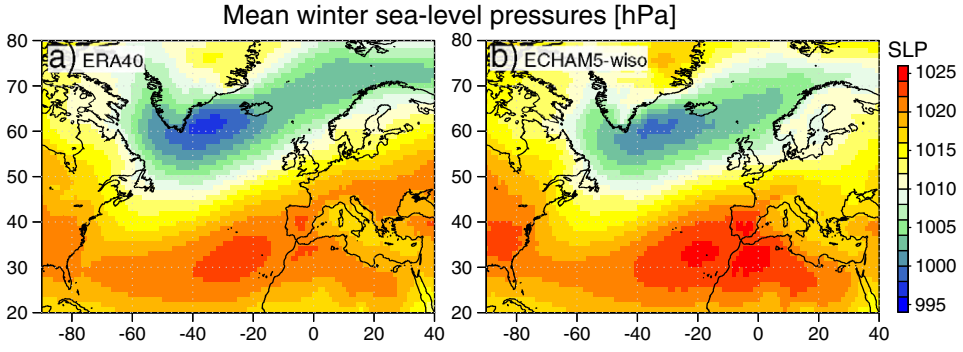

Fig. 4. Mean winter sea-level pressures over Europe from ERA40 (a) and ECHAM5-wiso (b). Results are averaged over 1959–1999.

Please cite this article as: Langebroek, P.M., et al., Climate information imprinted in oxygen-isotopic composition of precipitation in Europe, Earth Planet. Sci. Lett. (2011), doi:10.1016/j.epsl.2011.08.049

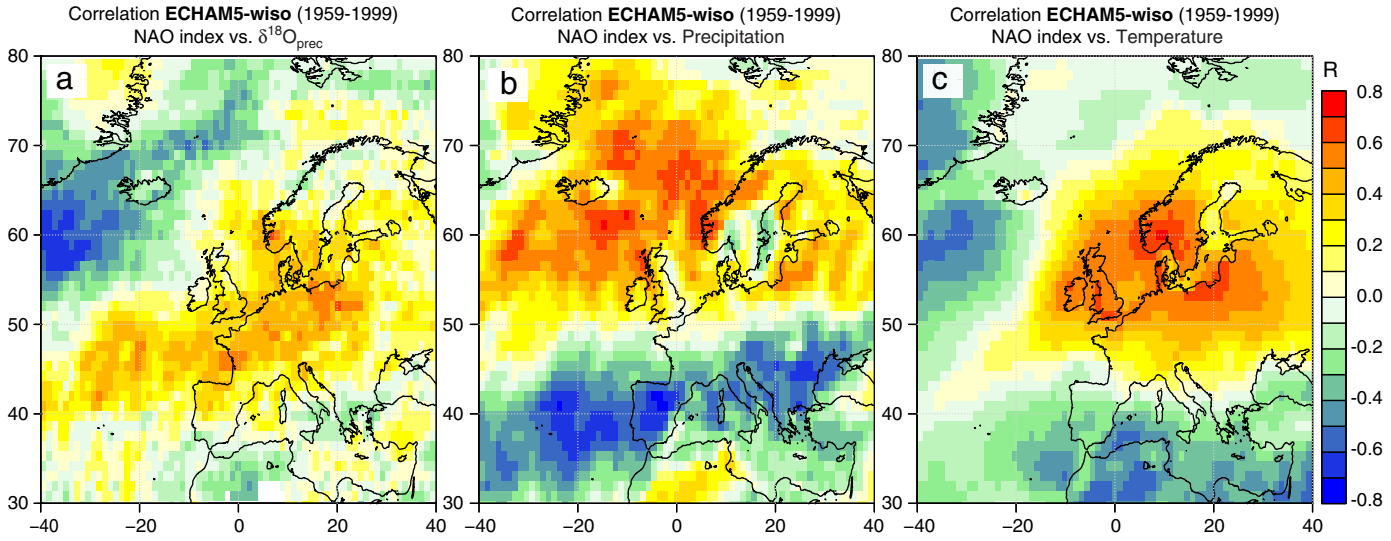

Fig. 5. Correlation maps of winter NAO index (see text) and winter mean $\delta^{18}O_{prec}$ values (a), precipitation (b) and temperature (c) using ECHAM5-wiso results for the period 1959–1999.

the observational data, it shows that ECHAM5-wiso captures the atmospheric dynamics explaining the data well. As a simple statistical downscaling approach, the correlations between the large-scale variables and the local climate can then be used to improve or even to predict the local temperature, precipitation or $\delta^{18}O_{prec}$ values.

4.1. Central Germany

Previously we showed that the NAO is best captured by the $\delta^{18}O_{prec}$ and temperature over western central Europe (Fig. 5). We therefore chose to further investigate the atmospheric circulation patterns affecting the local climate in this region. As an example, we focus more specifically on the Bunker Cave area, in central Germany (see Fig. 3 for location). Here we have the advantages of many local weather stations and three GNIP stations with a reasonably long record. The GNIP station data for Bad Salzuflen, Emmerich and Koblenz contain near-continuous coverage between 1980 and 1999. In order to explore the relationship between variations in $\delta^{18}O_{prec}$ from our example region and large-scale European climate, we first examine the GNIP and ECHAM5-wiso $\delta^{18}O_{prec}$ time series close to Bunker Cave (Fig. 6). The $\delta^{18}O_{prec}$ values of the three GNIP stations are precipitation-weighted and averaged into a composite record (Fig. 6a). All three stations contain data for most years. However, for some years values are missing, and then the composite record is based on two or even on one record. The measured values at these GNIP stations are relatively similar, although Emmerich has a tendency towards less depleted values. The mean values and standard deviations of the ECHAM5-wiso modeled (red) and the composite GNIP (black) $\delta^{18}O_{prec}$ records are very similar (Fig. 6b). T- and F-tests show that they are the statistically the same (confidence level of 95%). The data-model similarity is even greater if the marine-influenced Emmerich station is omitted from the composite data record. To estimate the model intrinsic $\delta^{18}O_{prec}$ variability for our simulation setup, we performed a second ECHAM5-wiso T106L31 simulation with the same AMIP-style forcing, only starting in 1977 (dashed red in Fig. 6b) instead of 1954. For the two model simulations the 20-year mean values and standard deviations are nearly identical (means of −9.79 and −9.71‰ and standard deviations of 1.19 and 1.15‰) and are therefore plotted as one model value. In contrast to the similarity in mean values, the pattern of interannual variability is different for the two model runs and the GNIP records. This is due to the internal variability in the system.

Next, we take advantage of the relatively long GNIP records available for the area around Bunker Cave and apply the proposed statistical downscaling to this region. Shifting the location of interest with a few degrees does not substantially alter the resulting patterns, indicating that the following results are representative for the entire central western Europe.

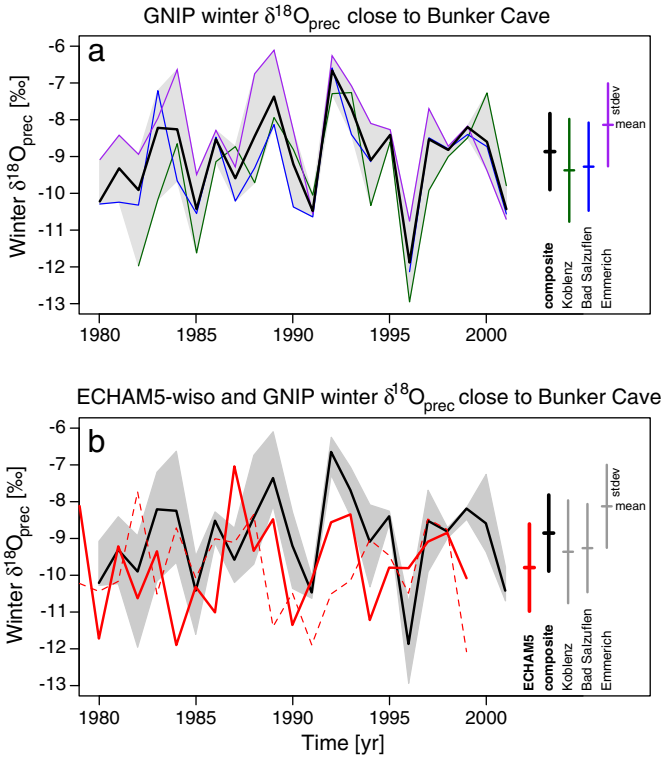

Fig. 6. Winter mean $\delta^{18}O_{prec}$ values close to Bunker Cave. (a) $\delta^{18}O_{prec}$ of the GNIP stations: Koblenz (green), Bad Salzuflen (blue), Emmerich (purple) and the composite record of the three GNIP stations (black). The gray shaded area indicates data range of the stations. (b) $\delta^{18}O_{prec}$ of the ECHAM5-wiso Bunker Cave grid box (red, alternative simulation in dashed red) on top of the range of the GNIP values from (a) (gray shaded area). 1-σ standard deviation and mean values are pointed out on the right side of the figures. The location of the three GNIP stations is shown in Fig. 3. (For interpretation of the references to color in this figure legend, the reader is referred to the web version of this article.)

Please cite this article as: Langebroek, P.M., et al., Climate information imprinted in oxygen-isotopic composition of precipitation in Europe, Earth Planet. Sci. Lett. (2011), doi:10.1016/j.epsl.2011.08.049

4.2. Correlation of local temperature to SLPs

For the time period 1959–1999 ERA40 temperatures near Bunker Cave show a strong anti-correlation with ERA40 SLP over the North Atlantic (Fig. 7a). The correlation of temperatures with SLP at Bunker Cave itself is close to zero, and a positive correlation is found for SLP over southern Europe and the Mediterranean. A similar dipole pattern is also found in the ECHAM5-wiso simulation for the modeled Bunker Cave temperature and sea-level pressure (Fig. 7b). The fact that the resulting correlation patterns resemble the NAO dipole pattern is in agreement with our previous results that central western European temperatures are strongly related to the NAO (Fig. 5c).

To investigate how well local Bunker Cave temperature is related to atmospheric circulation, we first take an areal mean of all SLPs in the region of highest correlation (Fig. 7a and b — white boxes) and compare them (winter by winter) to the local temperatures (Fig. 7c, black for ERA40 and red for ECHAM5-wiso values). The relationship between the Bunker Cave temperatures and the maximum correlated SLPs (white boxes) can then be described by linear regression equations (black and red lines in Fig. 7c):

$$\begin{aligned} T_{ERA40}(SLP_{ERA40})[^{\circ}C] &\approx -0.26\ SLP_{ERA40}[hPa] + 258 \\ {}_{TECHAM5}(SLP_{ECHAM5})[^{\circ}C] &\approx -0.24\ SLP_{ECHAM5}[hPa] + 239. \end{aligned} \quad (1)$$

The relationship is slightly stronger in the data than in the ECHAM5-wiso results (r^2 of 0.64 and 0.55, respectively), but the equations as well as the correlation patterns are very similar. On average ECHAM5-wiso computed slightly colder temperatures in the Bunker Cave region than observed (see also Fig. 2), which shifts the regression line towards lower temperatures with respect to the ERA40 regression line (Fig. 7c). We assessed the stability of these transfer functions by increasing or decreasing the area of maximum correlation considered (white boxes) by 2° in each direction. The resulting difference in correlation coefficient and regression line is very small ($\Delta r^2 \sim 0.004$; gray and light red lines in Fig. 7c).

Because of the robustness of the relationship, the ERA40-based T-SLP-relation can be used as a transfer function to calculate temperatures at Bunker Cave using ECHAM5-wiso SLP (Fig. 7d). The resulting calculated mean temperatures (blue lines) are higher than the directly modeled ECHAM5-wiso temperatures (red) and even slightly higher than the ERA40 temperatures at the cave site (black). Note that this type of statistical downscaling, using linear regression, always reduces the variance of the dataset.

The similarity in the correlation patterns (Fig. 7a and b) and transfer functions (Fig. 7c) of ERA40 and ECHAM5-wiso show that the model captures the temperature-SLP relationship in a realistic, NAO-like way. Thus, in a situation where only SLPs and no temperatures are available, the local temperature at Bunker Cave could be derived from the modeled (remote) SLP fields and the T-SLP relationship found in the ERA40 data (Eq. (1) and Fig. 7).

4.3. Correlation of local precipitation to SLPs

Local Bunker Cave precipitation can be correlated to SLP using the same technique as for temperature. The correlation patterns for the ERA40 data and ECHAM5-wiso results are relatively similar over Europe (Fig. 8a and b) although the correlation over North America differs. The precipitation at Bunker Cave is strongly anti-correlated to SLP in the Baltic Sea in both the data and the model results. Higher sea-level pressures over that region correspond to less precipitation at Bunker Cave.

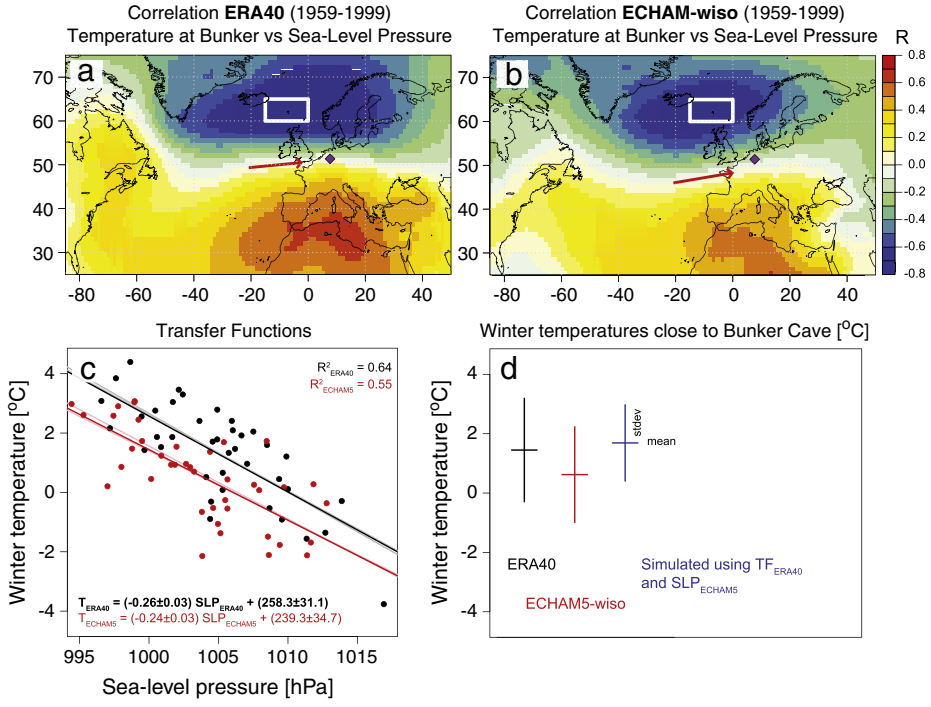

Fig. 7. Correlation map of winter temperature at Bunker Cave (purple diamond) and sea-level pressure fields using ERA40 data (a) and ECHAM5-wiso results (b) for the period 1959–1999. The white boxes indicate the region of highest correlation and the red arrows the direction of atmospheric circulation. (c) Correlation between sea-level pressures (from the white boxes in a and b) and Bunker Cave temperature for ERA40 (black) and ECHAM5-wiso (red). The linear regression line only slightly deviates when a 2° larger or smaller box is used (gray and light — red). (d) Mean values and 1-σ standard deviations of winter temperatures close to Bunker Cave for ERA40 (black), directly simulated by ECHAM5-wiso (red) and derived from the ERA40 transfer function (TF_{ERA40}) and ECHAM5-wiso sea-level pressure (blue) over the time period 1959–1999. (For interpretation of the references to color in this figure legend, the reader is referred to the web version of this article.)

Please cite this article as: Langebroek, P.M., et al., Climate information imprinted in oxygen-isotopic composition of precipitation in Europe, Earth Planet. Sci. Lett. (2011), doi:10.1016/j.epsl.2011.08.049

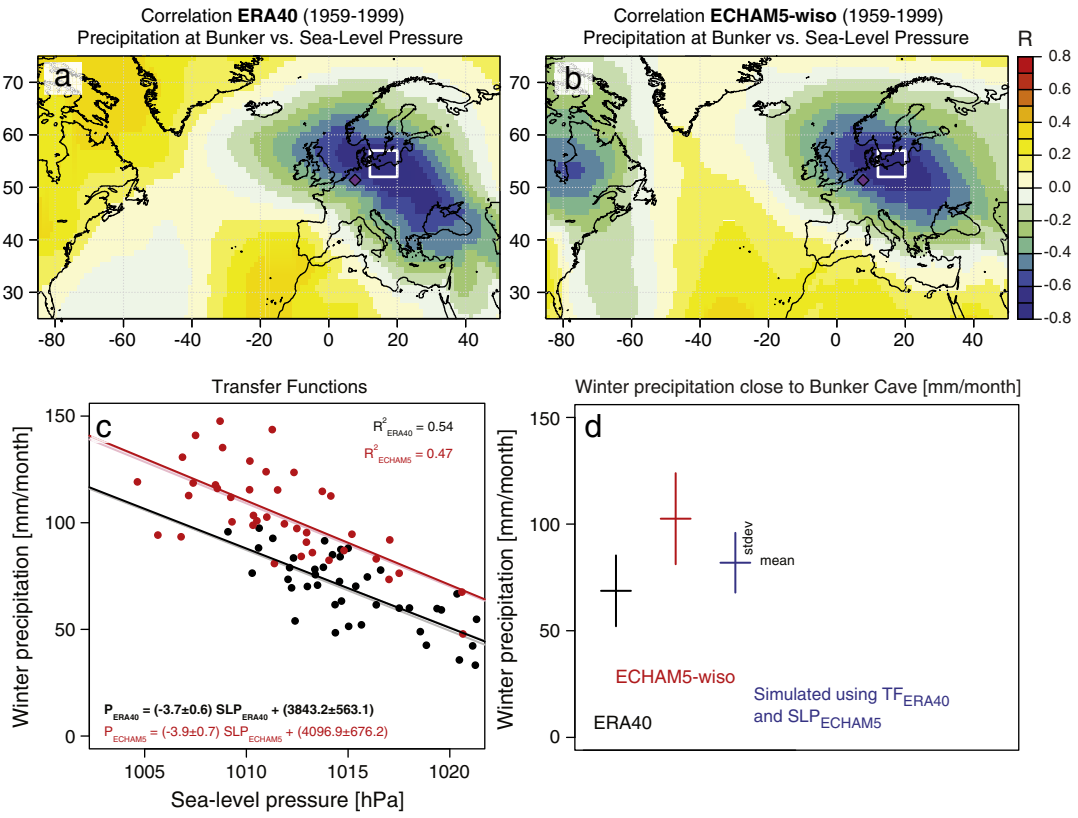

Fig. 8. As for Fig. 7, but for winter precipitation at Bunker Cave and sea-level pressure fields using ERA40 data and ECHAM5-wiso results.

The correlation patterns for Bunker Cave precipitation and SLP fields computed from ERA40 and ECHAM5-wiso differ from the typical NAO pattern and are related to an atmospheric flow from the northeast and a blocking pattern, similar to the Scandinavian or Eurasian-1 pattern described by Barnston and Livezey (1987). The similarity in the data and model correlation patterns indicate again common interannual variability of the atmospheric processes. We compare the local precipitation to its maximum correlated SLP (Fig. 8c) and retrieve the following linear regression equations:

$$P_{ERA40}(SLP_{ERA40})[mm/month] \approx -3.7\ SLP_{ERA40}[hPa] + 3843$$
$$P_{ECHAM5}(SLP_{ECHAM5})[mm/month] \approx -3.9\ SLP_{ERA40}[hPa] + 4097. \quad (2)$$

Again the relationship is very similar, but slightly stronger for the ERA40 data ($r^2 = 0.54$) than for the ECHAM5-wiso model ($r^2 = 0.47$). The higher modeled precipitation over the Baltic Sea (see Fig. 2) shifts the regression line to higher precipitation values (Fig. 8c – red). Also here we assessed the stability of the correlation by decreasing and increasing the area of maximum correlation (white boxes) by 2° in each direction. The resulting difference in correlation coefficient and regression line is again very small ($\Delta r^2 \sim 0.01$; gray and light red lines in Fig. 8c).

After applying the ERA40-based P-SLP-relation (Eq. (2)) on the ECHAM5-wiso SLPs in the Baltic Sea, we find a computed Bunker Cave precipitation (blue) with a mean value in between the originally computed ECHAM5-wiso (red) and ERA40 (black) precipitation (Fig. 8d), which shows that Bunker Cave winter precipitation can be derived from Baltic Sea winter SLPs.

4.4. Correlation of local $\delta^{18}O_{prec}$ to SLPs

Because the $\delta^{18}O_{prec}$ measurements close to Bunker Cave only cover the period between 1980 and 1999, we use the same technique as before with temperature and precipitation, but apply it over the shorter time span. The composite winter $\delta^{18}O_{prec}$ record of the three GNIP stations in the vicinity of Bunker Cave (Fig. 6 – black) is correlated to ERA40 SLP fields (Fig. 9a). In a comparable manner the Bunker Cave ECHAM5-wiso $\delta^{18}O_{prec}$ values are correlated to ECHAM5-wiso SLPs (Fig. 9b). The correlation maps look relatively similar and show a positive correlation to sea-level pressures over the western Mediterranean and a strong anti-correlation over eastern Scandinavia. Low pressures in the northeast combined with high pressures in the southwest result in less depleted $\delta^{18}O_{prec}$ values at Bunker Cave. Similar correlation patterns between central European $\delta^{18}O_{prec}$ values and SLPs using either GNIP stations and NCEP/NCAR reanalysis data or a low-resolution simulation of the NASA Goddard Institute for Space Studies Model E GCM were also reported by Field (2010). The SLPs in the maximum correlated region (white boxes) are again spatially averaged and plotted against $\delta^{18}O_{prec}$ values at Bunker Cave (Fig. 9c). The relationship is slightly more pronounced in the data than in the ECHAM5-wiso results ($r^2 = 0.59$ and $r^2 = 0.50$, respectively) and their linear regression lines are relatively similar:

$$\delta^{18}O_{prec\_GNIP}(SLP_{ERA40})[‰] \approx -0.17\ SLP_{ERA40}[hPa] + 164$$
$$\delta^{18}O_{prec\_ECHAM5}(SLP_{ECHAM5})[‰] \approx -0.15\ SLP_{ECHAM5}[hPa] + 146. \quad (3)$$

The apparent better agreement between these transfer functions compared to the T-SLP or P-SLP transfer functions is intriguing and might be due to the opposing effects of temperature and precipitation on $\delta^{18}O_{prec}$, smoothing out the climate signal. The exact size of the area of maximum correlation (white box) has again no major effect on the regression lines (gray and light red lines in Fig. 9c).

Applying the data-based $\delta^{18}O_{prec}$-SLP function (Eq. (3)) on the ECHAM5-wiso SLPs results in a simulated $\delta^{18}O_{prec}$ record which has a mean value and standard deviation similar to the originally GNIP and ECHAM5-wiso $\delta^{18}O_{prec}$ values (Fig. 9d). This transfer function

Please cite this article as: Langebroek, P.M., et al., Climate information imprinted in oxygen-isotopic composition of precipitation in Europe, Earth Planet. Sci. Lett. (2011), doi:10.1016/j.epsl.2011.08.049

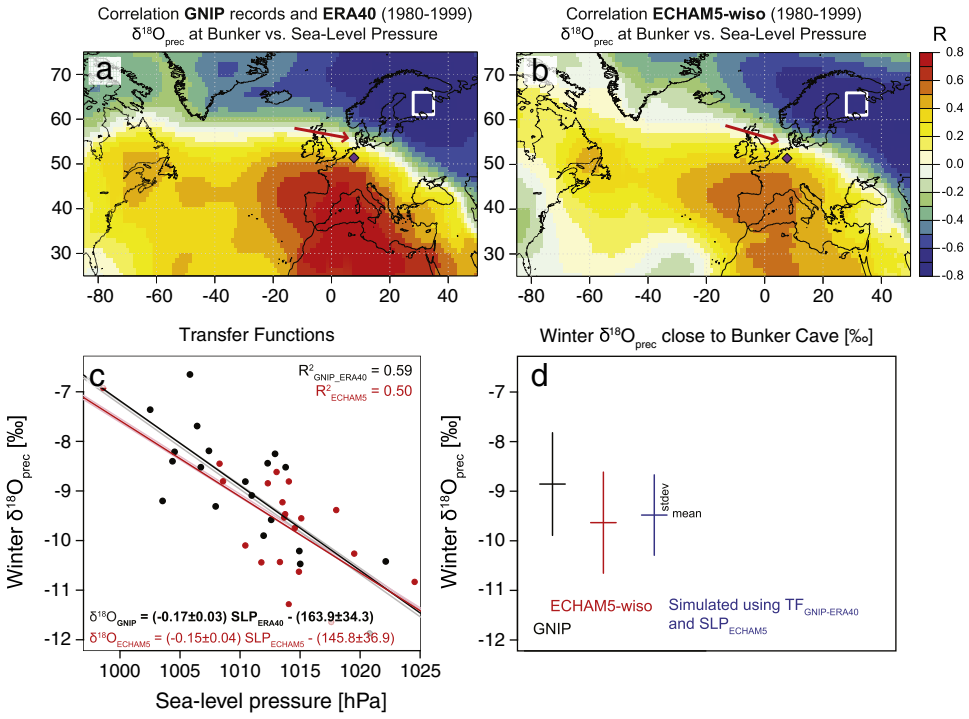

Fig. 9. As for Fig. 7, but for winter $\delta^{18}O_{prec}$ at Bunker Cave (GNIP composite record and ECHAM5-wiso) and sea-level pressure fields (ERA40 and ECHAM5-wiso).

can therefore be used to retrieve Bunker Cave $\delta^{18}O_{prec}$ from ERA40 or ECHAM5-wiso SLPs over eastern Scandinavia.

4.5. Correlation of local $\delta^{18}O_{prec}$ to other climate variables

Bunker Cave $\delta^{18}O_{prec}$ can also be correlated to large-scale European temperature (Fig. 10a and b) and precipitation (Fig. 10c and d) fields. The resulting correlation patterns resemble features of the NAO pattern: a north–south dipole over Europe for precipitation (Hurrell, 1995a; Hurrell and Deser, 2010) and a tripole temperature pattern in the North Atlantic (Deser and Blackmon, 1993; Dima and Lohmann, 2004). Both correlation patterns, however, are weaker than the correlation between $\delta^{18}O_{prec}$ at Bunker Cave and large-scale SLP fields (Fig. 9).

As the ECHAM5-wiso-based modeled $\delta^{18}O_{prec}$ values are very similar to the measured $\delta^{18}O_{prec}$ data around Bunker Cave, no transfer

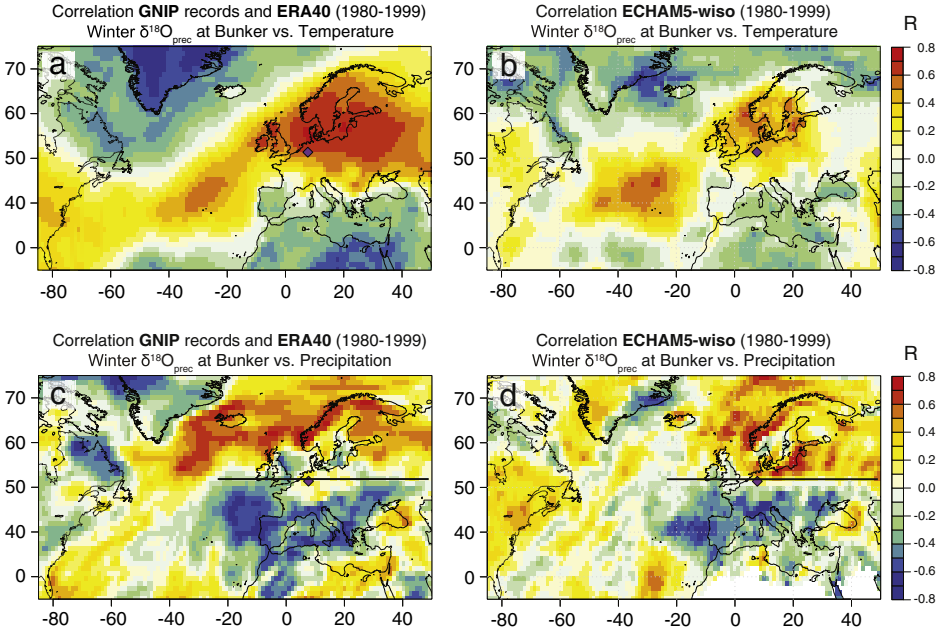

Fig. 10. Correlation maps of winter $\delta^{18}O_{prec}$ at Bunker Cave and large-scale temperature fields using the GNIP composite record (a) and ECHAM5-wiso results (b). Correlation maps of winter $\delta^{18}O_{prec}$ at Bunker Cave and large-scale precipitation fields using the GNIP composite record (c) and ECHAM5-wiso results (d). The horizontal lines indicate the dipole correlation pattern of $\delta^{18}O_{prec}$ at Bunker Cave and precipitation.

Please cite this article as: Langebroek, P.M., et al., Climate information imprinted in oxygen-isotopic composition of precipitation in Europe, Earth Planet. Sci. Lett. (2011), doi:10.1016/j.epsl.2011.08.049

function is needed in order to improve the values. However, if one uses a climate model without an explicit computation of $\delta^{18}O_{prec}$, it would be best to derive present-day winter $\delta^{18}O_{prec}$ values near Bunker Cave via an appropriate transfer function from SLP, and not directly from temperature or precipitation fields. This is true not only for Bunker Cave, but for the larger region of central western Europe (see also Field, 2010) and might be the same for other places in Europe. However, transfer functions should only be applied at locations without a high spatial heterogeneity, i.e. not in steep mountain ranges. Our findings support the results of Schmidt et al. (2007) that the isotopic composition of precipitation is in many cases a regionally integrated signal of several climate variables rather than a unique proxy for local changes of one particular climate variable.

5. Conclusions and outlook

Speleothem records in central western Europe indicate a dominant boreal winter influence (e.g., Wackerbarth et al., 2010). Motivated by this result, we evaluated the winter $\delta^{18}O_{prec}$ values, temperatures, precipitation amounts and sea-level pressures (SLP) of different datasets (GNIP, ERA40 and DWD) over Europe. We compared the available observational data to high-resolution simulation values from the atmospheric general circulation model ECHAM5, enhanced by explicit water isotope diagnostics (ECHAM5-wiso), and conclude the following:

(1) For the mean present-day climate (1959 to 1999), the simulated ECHAM5-wiso temperature, precipitation, $\delta^{18}O_{prec}$ values and sea-level pressures show the same distribution pattern over European as seen in the observational datasets.
(2) ECHAM5-wiso slightly underestimates the temperatures and overestimates the amounts of precipitation over Europe.
(3) Temperatures from local station data in central western Europe are well captured by the reanalysis dataset ERA40. In contrast, ERA40's precipitation lacks the high spatial heterogeneity found in local precipitation data.

In order to determine which climate variables are mostly NAO dominated and in which regions, we correlated an ECHAM5-wiso derived NAO index to modeled $\delta^{18}O_{prec}$, precipitation and temperature fields. Our ECHAM5-wiso results confirm the observation that NAO variability is most pronounced in $\delta^{18}O_{prec}$ and temperature time series in central Europe, as shown by Baldini et al. (2008) and Field (2010). In contrast, the NAO signature in modeled precipitation is best captured over the North Atlantic and Scandinavian latitudes or in southern Europe.

For an improved interpretation of $\delta^{18}O_{prec}$ variability as recorded in many paleoclimate records in Europe, the relationship between oxygen isotopes in precipitation, local climate changes and large-scale climate variability has to be quantitatively analyzed. Isotope-enabled climate models may help perform this task. As an example for such a quantitative analysis, we selected a site in central western Europe, where speleothem records are collected from the well-monitored cave within the DAPHNE project, Bunker Cave. In order to find the present-day atmospheric patterns influencing the $\delta^{18}O_{prec}$ record at Bunker Cave we performed correlation analyses between the local climate variables and large-scale climate changes on an interannual timescale. We find that:

(1) Local $\delta^{18}O_{prec}$, temperature and precipitation amount are strongly correlated to large-scale SLP fields (i.e. atmospheric circulation patterns) over western Europe and the North Atlantic in observational datasets. The ECHAM5-wiso model captures these relationships between local variables and remote SLP fields in a realistic manner.
(2) For temperature, the SLP-correlation resembles the NAO pattern. The relationship between precipitation and SLP is dominated by a blocking structure. The relation of $\delta^{18}O_{prec}$ with SLP shows a strong projection onto the NAO relation with temperature, although the northern center is shifted to the east.
(3) $\delta^{18}O_{prec}$ values at the Bunker Cave site are stronger correlated to SLP fields over western Europe and the North Atlantic than to temperature or precipitation fields over Europe.

In summary, our results indicate that variations of $\delta^{18}O$ in precipitation are rather a regionally integrated signal of several climate variables than a proxy for either local temperature or precipitation changes. This important conclusion is not just supported by our ECHAM5-wiso results or other modeling results (e.g., Schmidt et al., 2007), but is also confirmed by observational data (GNIP and ERA40).

This feature makes it especially attractive to use $\delta^{18}O$ records for reconstructing past large-scale circulation changes. High-resolution isotope data may even be used for synoptic scale features like blocking (Rimbu and Lohmann, 2010). For the Bunker Cave area the next step will be a coupling of the simulated ECHAM5-wiso atmospheric climate with an oxygen isotope drip water and stalagmite model (Wackerbarth et al., 2010). This will enable us to study the link between large-scale modes of variability (as NAO) to the local $\delta^{18}O$ signal archived in European speleothems.

One can furthermore argue that NAO-like large-scale changes detected in marine sediments (Rimbu et al., 2004) can be traced through boreal winter $\delta^{18}O$ signatures in central western Europe. However, this will be the subject of a subsequent study with our model.

Supplementary materials related to this article can be found online at doi:10.1016/j.epsl.2011.08.049.

Acknowledgments

This study is part of the DAPHNE Forschergruppe ('Dated speleothems archives of the paleoenvironment', DFG Forschergruppe 668), which is funded by the Deutsche Forschungsgemeinschaft. We thank the three anonymous reviewers and Gideon Henderson for their constructive comments.

References

Andersson, S., Rosqvist, G., Leng, M.J., Wastegård, S., Blaauw, M., 2010. Late Holocene climate change in central Sweden inferred from lacustrine stable isotope data. J. Quat. Sci. 25, 1305–1316.
Baldini, J.U.L., McDermott, F., Fairchild, I.J., 2006. Spatial variability in cave drip water hydrochemistry: implications for stalagmite paleoclimate records. Chem. Geol. 235, 390–404.
Baldini, L.M., McDermott, F., Foley, A.M., Baldini, J.U.L., 2008. Spatial variability in the European winter precipitation $\delta^{18}O$–NAO relationship: implications for reconstructing NAO-mode climate variability in the Holocene. Geophys. Res. Lett. 35, L04709. doi:10.1029/2007GL032027.
Barnston, A.G., Livezey, R.E., 1987. Classification, seasonality and persistence of low-frequency atmospheric circulation patterns. Mon. Weather. Rev. 115, 1083–1126.
Deser, C., Blackmon, M.L., 1993. Surface climate variations over the North Atlantic Ocean during winter: 1900–1989. J. Clim. 6, 1743–1753.
Deutscher Wetterdienst, t. Accessible at: http://www.dwd.de.
Dima, M., Lohmann, G., 2004. Fundamental and derived modes of climate variability: concept and application to interannual time-scales. Tellus 56A, 229–249.
Field, R., 2010. Observed and modeled controls on precipitation $\delta^{18}O$ over Europe: from local temperature to the Northern Annular Mode. J. Geophys. Res. 115, D12101. doi:10.1029/2009JD013370.
Gates, W.L., Boyle, J.S., Covey, C.C., Dease, C.G., Doutriaux, C.M., Drach, R.S., Fiorino, M., Gleckler, P.J., Hnilo, J.J., Marlais, S.M., Phillips, T.J., Potter, G.L., Santer, B.D., Sperber, K.R., Taylor, K.E., Williams, D.N., 1999. An overview of the results of the Atmospheric Model Intercomparison Project (AMIP I). Bull. Am. Meteorol. Soc. 80, 29–55.
Hagemann, S., Arpe, K., Roeckner, E., 2006. Evaluation of the hydrological cycle in the ECHAM5 model. J. Clim. 19, 3810–3827.
Hoffmann, G., Werner, M., Heimann, M., 1998. Water isotope module of the ECHAM atmospheric general circulation model — a study on timescales from days to several years. J. Geophys. Res. 103, 16871–16896.
Hurrell, J.W., 1995a. Decadal trends in the North Atlantic Oscillation: regional temperatures and precipitation. Science 269, 676–679.
Hurrell, J.W., 1995b. NAO Index Data Provided by the Climate Analysis Section. NCAR, Boulder, USA.

Hurrell, J.W., Deser, C., 2010. North Atlantic climate variability: the role of the North Atlantic Oscillation. J. Mar. Syst. 79, 231–244.
IAEA/WMO, 2006. Global Network of Isotopes in Precipitation. The GNIP Database. Accessible at: http://www.iaea.org/water. Data downloaded in 2010.
Jones, P.D., Jonsson, T., Wheeler, D., 1997. Extension of the North Atlantic Oscillation using early instrumental pressure observations from Gibraltar and south-west Iceland. Int. J. Climatol. 17, 1433–1450.
Joussaume, S., Sadourny, R., Jouzel, J., 1984. A general circulation model of water isotope cycles in the atmosphere. Nature 311, 24–29.
Jouzel, J., Russell, G.L., Suozzo, R.J., Koster, D., White, J.W.C., Broecker, W.S., 1987. Simulations of the HDO and $H_2^{18}O$ atmospheric cycles using the NASA GISS general circulation model: the seasonal cycle for present-day conditions. J. Geophys. Res. 92, 14739–14760.
Kress, A., Saurer, M., Siegwolf, R.T.W., Frank, D.C., Esper, J., Bugmann, H., 2010. A 350 year drought reconstruction from Alpine tree ring stable isotopes. Glob. Biogeochem. Cycles 24, GB2011. doi:10.1029/2009GB003613.
Lachniet, M.S., 2009. Climatic and environmental controls on speleothem oxygen-isotope values. Quat. Sci. Rev. 28, 412–432.
LeGrande, A.N., Schmidt, G.A., 2006. Global gridded data set of the oxygen isotopic composition in seawater. Geophys. Res. Lett. 33, L12604. doi:10.1029/2006GL026011.
McDermott, F., 2004. Palaeo-climate reconstruction from stable isotope variations in speleothems: a review. Quat. Sci. Rev. 23, 901–918.
Petit, J.R., Jouzel, J., Raynaud, D., Barkov, N., Barnola, J.M., Basile, I., Bender, M., Chappellaz, J., Davis, M., Delaygue, G., Masson-Delmotte, V., Kotlyakov, V., Legrand, M., Lipenkov, V., Lorius, C., Pepin, L., Ritz, C., Saltzman, E., Stievenardt, M., 1999. Climate and atmospheric history of the past 420,000 years from the Vostok ice core, Antarctica. Nature 399, 429–436.
Randall, D.A., Wood, R.A., Bony, S., Colman, R., Fichefet, T., Fyfe, J., Kattsov, V., Pitman, A., Shukla, J., Srinivasan, J., Stouffer, R., Sumi, A., Taylor, K., 2007. In: Solomon, S., Qin, D., Manning, M., Chen, Z., Marquis, M., Averyt, K., Tignor, M., Miller, H. (Eds.), Climate Change 2007: The Scientific Basis. Contribution of Working Group 1 to the Fourth Assessment Report of the Intergovernmental Panel on Climate Change. Cambridge University Press, Cambridge, United Kingdom and New York, NY, USA, p. 881.
Riechelmann, D.F.C., 2010. Aktuospeläologische Untersuchungen in der Bunkerhöhle des Iserlohner Massenkalks (NRW/Deutschland): Signifikanz für kontinentale Klimaarchive. Ph.D. thesis. Ruhr-University Bochum, Germany, In German.
Rimbu, N., Lohmann, G., 2010. Decadal variability in a central Greenland high-resolution deuterium isotope record and its relationship to the frequency of daily atmospheric circulation patterns from the North Atlantic region. J. Clim. 23, 4608–4618.
Rimbu, N., Lohmann, G., Lorenz, S.J., Kim, J.H., Schneider, R.R., 2004. Holocene climate variability as derived from alkenone sea surface temperature and coupled ocean–atmosphere model experiments. Clim. Dyn. 23, 215–227.
Roeckner, E., Bäuml, G., Bonaventura, L., Brokopf, R., Esch, M., Giorgetta, M., Hagemann, S., Kirchner, I., Kornblueh, L., Manzini, E., Rhodin, A., Schlese, U., Schulzweida, U., Tompkins, A., 2003. The Atmospheric General Circulation Model ECHAM5. Part I: Model Description. Technical Report. Max Planck Institute for Meteorology. MPI-Report 349.
Roeckner, E., Brokopf, R., Esch, M., Giorgetta, M., Hagemann, S., Kornblueh, L., Manzini, E., Schlese, U., Schulzweida, U., 2006. Sensitivity of simulated climate to horizontal and vertical resolution in the ECHAM5 atmosphere model. J. Clim. 19, 3771–3791.
Rozanski, K., Araguás-Araguás, L., Gonfiantini, R., 1993. Relation between long-term trends of oxygen-18 isotope composition of precipitation and climate. Science 258, 981–985.
Schmidt, G.A., LeGrande, A.N., Hoffmann, G., 2007. Water isotope expressions of intrinsic and forced variability in a coupled ocean–atmosphere model. J. Geophys. Res. 112, D10103. doi:10.1029/2006JD007781.
Uppala, S.M., Kållberg, P.W., Simmons, A.J., Andrae, U., da Costa Bechtold, V., Fiorino, M., Gibson, J.K., Haseler, J., Hernandez, A., Kelly, G.A., Li, X., Onogi, K., Saarinen, S., Sokka, N., Allan, R.P., Andersson, E., Arpe, K., Balmaseda, M.A., Beljaars, A.C.M., van de Berg, L., Bidlot, J., Bormann, N., Caires, S., Chevallier, F., Dethof, A., Dragosavac, M., Fisher, M., Fuentes, M., Hagemann, S., Hólm, E., Hoskins, B.J., Isaksen, L., Janssen, P.A.E.M., Jenne, R., McNally, A., Mahfouf, J.F., Morcrette, J.J., Rayner, N.A., Saunders, R.W., Simon, P., Sterl, A., Trenberth, K.E., Untch, A., Vasiljevic, D., Viterbo, P., Woollen, J., 2005. The ERA-40 re-analysis. Q. J. R. Meteorol. Soc. 131, 2961–3012.
Wackerbarth, A., Scholz, D., Fohlmeister, J., Mangini, A., 2010. Modelling the $\delta^{18}O$ value of cave drip water and speleothem calcite. Earth Planet. Sci. Lett. 299, 387–397.
Walker, G.T., Bliss, E.W., 1932. World weather V. Mem. R. Meteorol. Soc. 4, 53–84.
Werner, M., Langebroek, P.M., Carlsen, T., Herold, M., Lohmann, G., 2011. Stable water isotopes in the ECHAM5 general circulation model: towards high resolution isotope modelling on a global scale. J. Geophys. Res. 116, D15109. doi:10.1029/2011JD015681.

Please cite this article as: Langebroek, P.M., et al., Climate information imprinted in oxygen-isotopic composition of precipitation in Europe, Earth Planet. Sci. Lett. (2011), doi:10.1016/j.epsl.2011.08.049